

Structural Phase Transitions in $(n\text{-C}_3\text{H}_7\text{NH}_3)_2\text{SbBr}_5$

R. Jakubas and G. Bator

Institute of Chemistry, University of Wrocław, Joliot-Curie 14, 50 383 Wrocław, Poland

M. Foulon and J. Lefebvre

Laboratoire de Dynamique et Structures des Matériaux Moléculaires (U.A. No 801),
UFR de Physique, Université de Lille I, 59 655 Villeneuve d'Ascq Cédex, France

J. Matuszewski

Department of Inorganic Chemistry, Faculty of Engineering, School of Economics,
50 345 Wrocław, Poland

Z. Naturforsch. **48a**, 529–534 (1993); received October 7, 1992

Dielectric, DSC, thermal expansion and preliminary X-ray diffraction studies on $(n\text{-C}_3\text{H}_7\text{NH}_3)_2\text{SbBr}_5$ are reported. It was found that this crystal undergoes a complex sequence of phase transitions. On cooling: phase I → phase II at 188.7 K (continuous), II → III at 165 K (1st order, $\Delta S = 26.8 \text{ J/mol K}$), III → IV at 137 K (1st order, 1.6 J/mol K). On heating: IV → III at 154 K, III → II' at 168 K, II' → II at 177 K (1st order, 2.8 J/mol K), II → I at 189 K. All 1st order phase transitions are likely due to the motion of the $n\text{-C}_3\text{H}_7\text{NH}_3^+$ cations. The dielectric dispersion studies between 100 Hz–1 MHz within the phases I and II indicate a fast reorientational motion of dipoles with $\tau < 10^{-7} \text{ s}$.

Key words: Alkylammonium halogenoantimonates, Phase transition, Dielectric, DSC, Thermal expansion

1. Introduction

The properties of crystals of the family of alkylammonium halogenoantimonates (III) with the general formula $\text{R}_3\text{M}_2\text{X}_9$ (where $\text{R} = (\text{CH}_3)_n\text{NH}_4 - n$, $\text{M} = \text{Sb, Bi, X} = \text{Cl, Br, I}$) have been extensively investigated, cf. [1–4] and references cited therein. Most of these compounds revealed pyroelectricity [5], ferroelectricity [6] and ferroelasticity [7]. Motions of the alkylammonium cation induce order-disorder type phase transitions.

Ferroelectric properties have also been found in the closely related crystals of $(\text{CH}_3\text{NH}_3)_5\text{Bi}_2\text{X}_{11}$ ($\text{X} = \text{Cl, Br}$) [1]. In general, the structure and physical properties of $\text{R}_x\text{M}_y\text{X}_z$ (where $\text{R} = \text{alkylammonium}$) complexes are affected by the size and symmetry of the cations. Very little is known about possible structural phase transitions in such crystals containing larger alkylammonium cations than $(\text{CH}_3)_n\text{NH}_4^+ - n$ ones.

Recently NQR on $(n\text{-C}_3\text{H}_7\text{NH}_3)_2\text{SbBr}_5$ has revealed a disappearance of resonance lines above 160 K

[8]. DTA on this crystal corroborates the structural phase transition (SPT) of 1st order at 170 K. The crystal structure is bis-*n*-propylammonium pentabromoantimonate (hereafter abbreviated as nPBA has not been reported as yet.

To clarify the features of the transition, we have carried out X-ray (at room temperature), thermal expansion, DSC and dielectric measurements.

2. Experimental

2.1. Samples

nPBA was obtained by slow evaporation of an aqueous solution containing stoichiometric amounts of propylamine and Sb_2O_3 with an excess of HBr. Single crystals were grown by slow evaporation of an aqueous solution at room temperature. Platelet-shaped single crystals of about $5 \times 5 \times 1 \text{ mm}^3$ were used for the dielectric measurements between 170–300 K; silver paste was used as the electrodes.

Single crystals are completely destroyed at the 165 K phase transition (PT) point. To perform measurements below 165 K, polycrystalline samples of about $50 \text{ mm}^2 \times 1 \text{ mm}$ were formed from a powder.

Reprint requests to Dr. R. Jakubas, Institute of Chemistry, University of Wrocław, Joliot-Curie 14, 50 383 Wrocław, Poland.

0932-0784 / 93 / 0300-0529 \$ 01.30/0. – Please order a reprint rather than making your own copy



Dieses Werk wurde im Jahr 2013 vom Verlag Zeitschrift für Naturforschung in Zusammenarbeit mit der Max-Planck-Gesellschaft zur Förderung der Wissenschaften e.V. digitalisiert und unter folgender Lizenz veröffentlicht: Creative Commons Namensnennung-Keine Bearbeitung 3.0 Deutschland Lizenz.

Zum 01.01.2015 ist eine Anpassung der Lizenzbedingungen (Entfall der Creative Commons Lizenzbedingung „Keine Bearbeitung“) beabsichtigt, um eine Nachnutzung auch im Rahmen zukünftiger wissenschaftlicher Nutzungsformen zu ermöglichen.

This work has been digitized and published in 2013 by Verlag Zeitschrift für Naturforschung in cooperation with the Max Planck Society for the Advancement of Science under a Creative Commons Attribution-NoDerivs 3.0 Germany License.

On 01.01.2015 it is planned to change the License Conditions (the removal of the Creative Commons License condition "no derivative works"). This is to allow reuse in the area of future scientific usage.

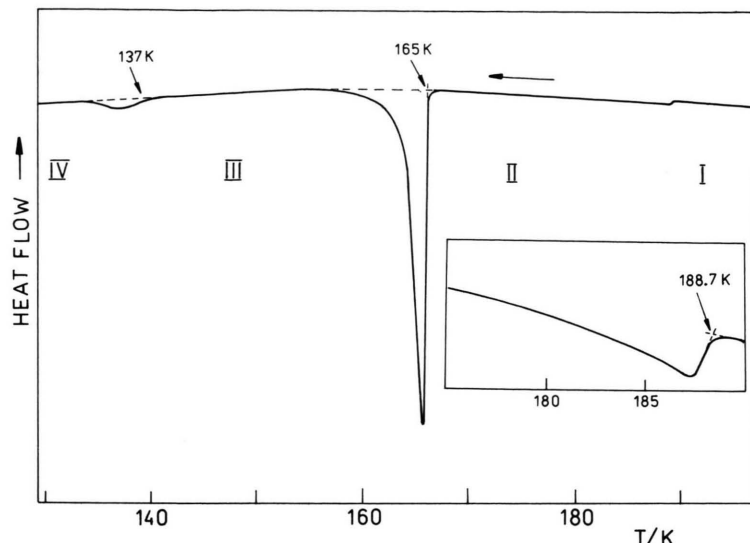


Fig. 1. Differential scanning calorimeter curves of nPBA on cooling (3 K/min).

2.2. DSC Measurements

The calorimetric measurements were performed on a Perkin-Elmer DSC-7 differential scanning calorimeter with a scanning speed of 3 deg/min.

2.3. Thermal Expansion

The linear thermal expansion was measured by a dilatometer of the difference transformer type (thermo-mechanical analyzer Perkin-Elmer TMS-2). Under dynamic temperature conditions the measurements were performed on heating and cooling at rates of 0.1–0.15 K/min. The measurements on each sample were repeated several times. The results were reproducible within 10–15%. The accuracy of the thermal expansion determination is about 2%.

2.4. Dielectric Measurements

The complex electric permittivity ϵ^* was measured by means of an HP 4284A precision LCR meter from 100 Hz to 1 MHz and in the temperature range from about 300 K to 100 K, the cooling rate being about 0.1 K/min in the vicinity of the critical temperature (T_c) and about 1 K/min elsewhere.

2.5. X-ray Experiment

The single crystal data were obtained using a commercial Weissenberg camera (Cu-K_α , $\lambda = 1.54184 \text{ \AA}$).

3. Results and Discussion

3.1. X-ray Diffraction Studies

Preliminary X-ray crystal studies were not successful since even very small single crystals grown from aqueous solution exhibited multiple twinning along the a -axis. Therefore the space group determination was not feasible. The presented crystal data combine the results of "single" crystal oscillation photograph results and powder diffraction data. The latter were used for indexing procedures (ITO, Powder routines) as well as for the refinement of the unit cell parameters. It should be stressed that the indexation of the powder data was not unique and led to several solutions with very close figures of merit. The most probable solution has been selected by direct comparison with the b and c directions found from oscillation photographs.

The reflections were indexed on an orthorhombic unit cell (primitive). The following lattice parameters at room temperature (295 K) were obtained: $a = 7.884(7)$, $b = 14.516(7)$, $c = 15.913(9) \text{ \AA}$ ($V = 1821.1 \text{ \AA}^3$), $Z = 4$, $d_m = 2.33$, $d_c = 2.3(4)$.

3.2. DSC Results

DSC experiments have been performed on heating and cooling between 100 and 300 K. In Fig. 1 a cooling run at 3 K/min is shown. From the DSC plot it follows that nPBA undergoes, on cooling, three suc-

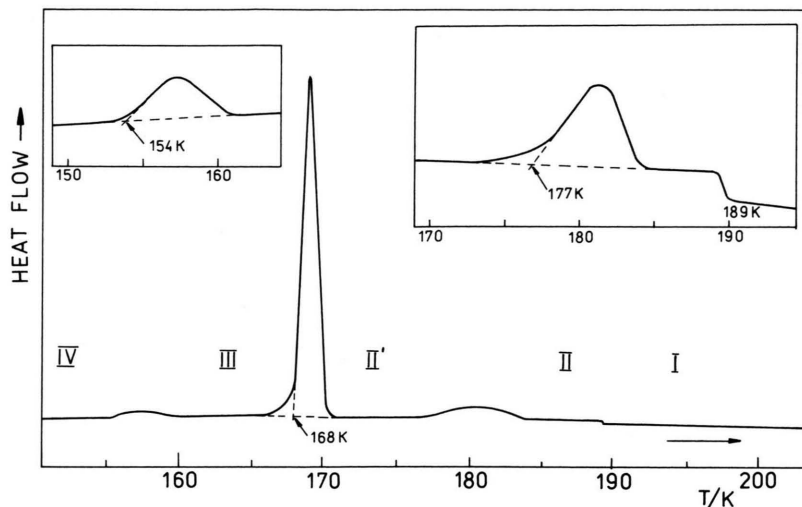


Fig. 2. Differential scanning calorimeter curves of nPBA on heating (3 K/min).

Table 1. Phase transitions in $(n\text{-C}_3\text{H}_7\text{NH}_3)_2\text{SbBr}_5$.

Cooling			Heating		
Type of PT	T_c [K]	ΔS [J/mol K]	Type of PT	T_c [K]	ΔS [J/mol K]
I → II 2nd order	188.7	—	II → I 2nd order	189	—
II → III 1st order	165	26.8	II' → II 1st order	177	2.8
III → IV 1st order	137	1.6	III → II' 1st order	168	25.2
			IV → III 1st order	154	1.5

cessive structural phase transitions. Unexpectedly, on heating from 100 K (see Fig. 2) nPBA reveals an additional heat anomaly between the phases III and II.

The obtained parameters of all heat anomalies are listed in Table 1.

The largest heat anomalies at the II → III and III → II' PT's correspond to the PT visible by NQR and DTA techniques [8]. Note the relatively large transition entropy (about 13 J/mol K per cation) at 165 K. The continuous I → II PT at 188.7 K and 1st order III → IV PT at 137 K are reported here for the first time. The latter one is characterized by a relatively small associated entropy change (1.6 J/mol K) but a distinct temperature hysteresis of the order of 17 K. The 1st order II' → II PT at 177 K is irreversible and visible only during heating.

The DSC studies seem to suggest that the transition from the phases III to II proceeds by the formation of the metastable phase II'.

The entropy values obtained for all 1st order PTs in nPBA indicate the order-disorder type of these transformations. However, the III → IV PT is likely due to a subtle structural change.

3.3. Thermal Expansion

The overall behaviour of the thermal dilation of polycrystalline nPBA on cooling is shown in Figure 3. Distinct anomalies in the thermal dilation occur at T_{c2} (162 K) and T_{c3} (134 K), indicating the 1st order PT which is consistent with that found by DSC. It should be noted that the II → III PT is accompanied by a relatively large expansion ($\Delta l/l \approx 1 \cdot 10^{-2}$). Because of the cracks of the sample at this transition point the observed jump of $\Delta l/l$ may be regarded as qualitative. The next jump of $\Delta l/l$ at T_{c3} (III → IV) of about $1.4 \cdot 10^{-3}$ was very well reproducible. The insert in Fig. 3 shows in detail the changes in the expansion curve near the I → II PT and corroborates the 2nd order nature of this transition. Figure 4 shows the temperature dependence of dilation of polycrystalline nPBA on heating. The value of the first anomaly at T_{c3} is comparable with that on cooling, but the next one at T_{c2} is distinctly smaller on heating than $(\Delta l/l)_{162\text{ K}}$ on cooling. It is interesting that the additional PT at T_{c2} reveals the opposite sign in the change of $\Delta l/l$ in comparison to the two first PT's. The con-

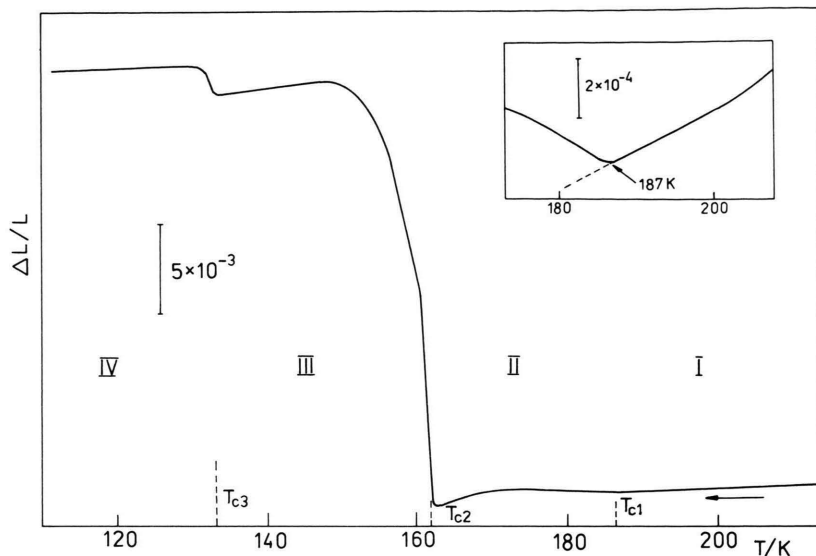


Fig. 3. Thermal expansion of polycrystalline nPBA on cooling.

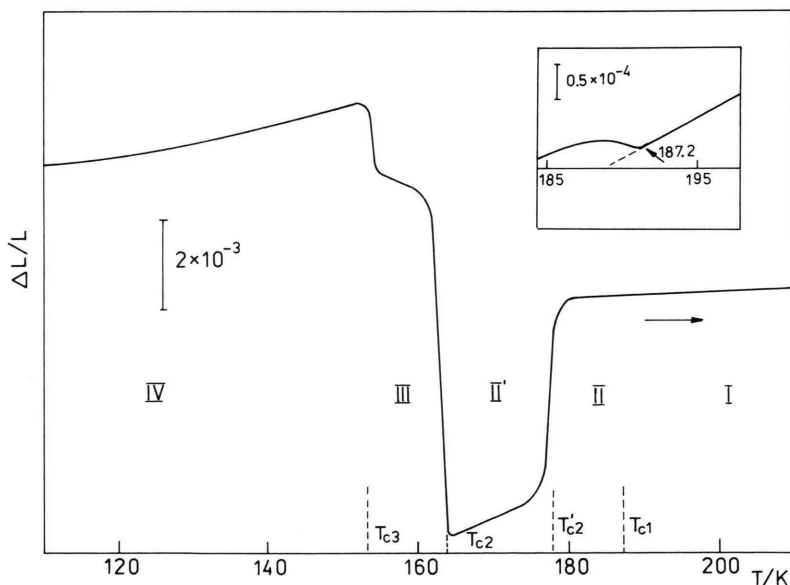


Fig. 4. Thermal expansion of polycrystalline nPBA on heating.

tinuous PT at T_{c1} is well visible (see the insert in Figure 4). For the III \rightarrow IV PT, which is well reproducible, one can estimate the pressure coefficient using the Clausius-Clapeyron relation

$$dT_c/dp = \Delta V/\Delta S,$$

where $\Delta V = 3 \times \Delta l/l$ is the change in molar volume at T_{c3} and ΔS is the entropy change estimated from our DSC experiment. The obtained value of dT_c/dp is $76.5 \cdot 10^{-2} \text{ K} \cdot \text{MPa}^{-1}$.

Summarizing the thermal expansion studies, one can state that the present dilatometric experiment corroborates both the sequence and the nature of the PTs detected by DSC technique.

3.4. Dielectric Results

The dielectric measurements were performed both for the polycrystalline and for the single crystal samples in the c -axis direction, which seemed to be the most interesting one.

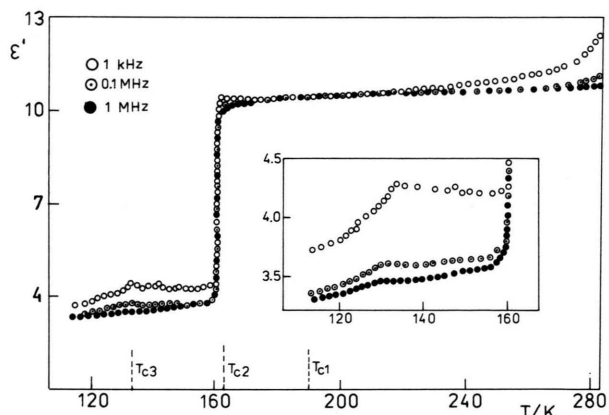


Fig. 5. Temperature dependence of the electric permittivity ϵ' of polycrystalline nPBA at various frequencies between 285–115 K.

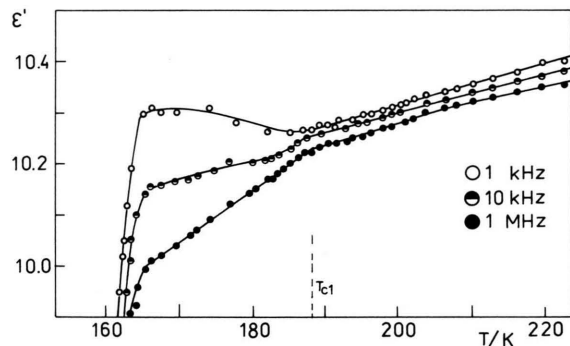


Fig. 6. Temperature dependence of the electric permittivity ϵ' of polycrystalline nPBA at various frequencies in the vicinity of I \rightarrow II PT and II \rightarrow III PT points.

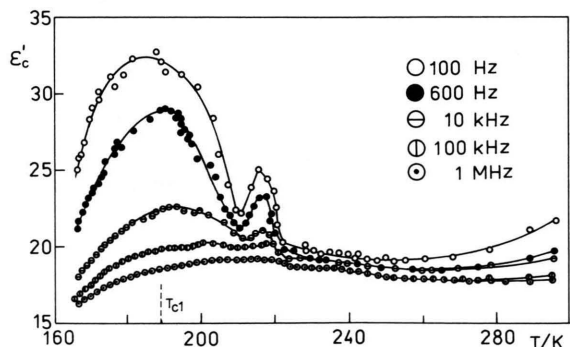


Fig. 7. Temperature dependence of the electric permittivity ϵ' along the c -axis of nPBA in the vicinity of the I \rightarrow II PT temperature.

Figure 5 shows the temperature dependence of the electric permittivity ϵ' (the results were obtained for the frequency range 100 Hz–1 MHz) for a few selected frequencies in the whole temperature interval. The crystal of nPBA exhibits a certain dispersion of permittivity ϵ^* at room temperature, the strength of which within the phase I decreases with decreasing temperature. The permittivity in this phase is fairly constant (11 units) and decreases negligibly down to the first phase transition at 188 K, which is in detail illustrated in Figure 6. Below 188 K the temperature dependence of ϵ' changes. At the lowest frequencies a slight increase of ϵ' with decreasing temperature is observed. On the other hand at the highest frequencies a visible change in the slope of the linear dependence of $\epsilon'(T)$ occurs. At the II \rightarrow III PT a drastic jump of the permittivity (near 7 units) is observed (see Fig. 5), the temperature characteristic resembling to some extent a phase transition of the "rotational" type. After the transformation to the phase III the samples crack and the observed dielectric picture is only qualitative (see insert in Figure 5). Nevertheless, in the vicinity of 135 K an anomaly is visible with a broad ϵ' maximum. Dispersion of the permittivity in this frequency region for the phase IV might be expected.

More interesting results were obtained from the measurements of the single crystals. At room temperature (290 K) the nPBA crystal exhibits a distinct anisotropy of the dielectric properties, $\epsilon'_a \approx 12$, $\epsilon'_c \approx 19$. A preparation of corresponding samples perpendicularly to the b -direction did not succeed (two cleavage planes).

Starting from room temperature, ϵ' at all used frequencies decreases slightly with temperature, but below 260 K it increases. Close to 220 K (for most of investigated single crystals) a step-wise change of ϵ' is observed, particularly well seen at low frequencies. It should be mentioned that no effect close to 220 K for the polycrystalline samples was observed. The reason for this behaviour is not clear, and the DSC and dilatometric studies did not record any essential thermal anomaly in this temperature range. Furthermore, a distinct temperature anomaly with strong frequency dependence of $\epsilon'(\omega)$ is observed close to 190 K, which corresponds to the continuous I \rightarrow II PT. The dielectric losses accompanying this phase transition are significantly lower, which indicates the strong broadening of the observed dispersion of $\epsilon^*(\omega)$.

A discussion of the observed PTs requires the knowledge of the crystal structure of the compound under study to define the type of ordering of the n-propyl-

ammonium cation. It is, however, undoubtful (taking into account the entropy values ΔS) that this cation contributes essentially to all the structural PTs. The dielectric picture in the vicinity of the T_c of II \rightarrow III seems unexpected. The “rotational” type of the $\epsilon'(T)$ characteristic requires a sudden freezing of the whole or part of the molecule with a significant dipole moment. Additionally, it should be noticed that dielectric dispersion related to this motion, above T_{c2} , should be found at frequencies higher than 1 MHz. This motion is therefore relatively fast. A similar dielectric response was also encountered in crystals of $(\text{CH}_3\text{NH}_3)_3\text{M}_2\text{X}_9$ ($\text{M} = \text{Sb, Bi}$; $\text{X} = \text{Cl, Br, I}$), where the methylammonium cation performed the isotropic rotation. Since it is least probable that the *n*-propylammonium cation performs the isotropic motion as a whole, only the rotation of part of it can give a contribution to the mechanism of the II \rightarrow III PT. The mechanism of the continuous I \rightarrow II transition may be more complex. The low frequency process (in the kilohertz region) plays undoubtly a role here. The magnitude of this process is, however, significantly distorted by the permittivity anomaly at 220 K, particularly at low frequencies.

Dielectric studies on single crystals for all crystallographic directions are now in progress. Careful X-ray investigations are also necessary in order to elucidate the origin of all transitions.

4. Conclusions

1. $(n\text{-C}_3\text{H}_7\text{NH}_3)_2\text{SbBr}_5$ belongs to the orthorhombic symmetry at room temperature.
2. Both DSC and thermal expansion studies revealed the structural phase transitions in nPBA for the first time:
 - a) continuous PT at 188.7 K/189 K (cooling/heating),
 - b) 1st order PT at 137 K/154 K,
 - c) 1st order PT at 177 K (irreversible, only on heating).
3. All 1st order PTs are accompanied with large entropy changes, indicating an order-disorder mechanism likely due to *n*-propylammonium cation disorder.
4. From the dielectric point of view the II \rightarrow III PT is a typical 1st order transition related to a freezing of rotational motion (like a plastic molecular crystal). This transformation should be due to a drastic structural change.
5. The lack of a distinct dielectric dispersion of ϵ^* within the phases I and II up to 1 MHz points to a very fast reorientational motion of dipoles connected with $n\text{-C}_3\text{H}_7\text{NH}_3^+$ cations ($\tau < 10^{-7}$ s).
6. A distinct anisotropy of the electric permittivity ($\epsilon'_c > \epsilon'_a$) is found in the room temperature phase I.

- [1] R. Jakubas and L. Sobczyk, *Phase Transitions* **20**, 163 (1990).
- [2] H. Ishihara, K. Watanabe, A. Iwata, K. Yamada, Y. Kinosita, T. Okuda, V. G. Krishnan, S. Dou, and A. Weiss, *Z. Naturforsch.* **47a**, 65 (1992).
- [3] M. Maćkowiak, N. Weiden, and A. Weiss, *Phys. Stat. Sol. (a)* **119**, 77 (1990).
- [4] P. Koziol, Y. Furukawa, and D. Nakamura, *J. Phys. Soc. Japan* **60**, 3850 (1991).
- [5] J. Zaleski, R. Jakubas, L. Sobczyk, and J. Mróz, *Ferroelectrics* **103**, 83 (1990).
- [6] R. Jakubas, U. Krzewska, G. Bator, and L. Sobczyk, *Ferroelectrics* **77**, 129 (1988).
- [7] J. Zaleski, R. Jakubas, and L. Sobczyk, *Phase Transitions* **27**, 25 (1990).
- [8] T. Okuda, N. Tanaka, S. Ichiba, and K. Yamada, *Z. Naturforsch.* **41a**, 319 (1986).